Electron Transfer Collisions with Oriented Trifluoroacetic Acid (CF_3CO_2H)†

Philip R. Brooks*

Chemistry Department and Rice Quantum Institute, Rice University Houston, Texas 77005

Received: March 31, 2009; Revised Manuscript Received: July 12, 2009

Electron transfer collisions between neutral K atoms and neutral, oriented trifluoroacetic acid molecules, CF_3CO_2H, are studied in crossed molecular beams at center of mass energies from 6 to 18 eV. An electron transfer produces a pair of ions with enough energy to escape the Coulomb attraction, and the ions are detected in separate time-of-flight mass spectrometers. The principle ions formed are K^+ and the trifluoroacetate ion, $CF_3CO_2^-$ ion, and this channel is favored for attack at the positive ($-CO_2H$) end of the molecule. The steric asymmetry suggests that the electron is transferred into the π^*_{CO} orbital. The nascent K^+ perturbs the molecular symmetry, allowing electron migration to the σ^*_{OH} orbital to break the O−H bond and form $CF_3CO_2^-$.

Introduction

Very low energy electrons are amazingly destructive to biological molecules.[1,2] Formic and acetic acid, prototypes for more complex amino acids, attach electrons in a resonance near 1.3 eV and dissociate to produce a reactive H atom and a negative carboxylate ion.[3−8] The attachment of free electrons to carboxylic acids has generally been thought to occur via a π^*_{CO} shape resonance, but this interpretation has recently been questioned[9] with the suggestion that the electron is attached via a very broad, higher energy, σ^*_{OH} shape resonance. If the electron attaches to the σ^*_{OH} orbital, the OH bond can directly dissociate, but if the electron enters the π^* orbital of A″ symmetry, it must migrate to the σ^*_{OH} orbital of A′ symmetry to break the OH bond. Recent calculations[10] show that the A″−A′ symmetry can be broken by molecular vibrations.

We recently studied electron transfer to acetic acid molecules oriented before the collision.[11] Attacking the CO_2H end of the molecule produces the largest acetate ion signal. The steric asymmetry is small and independent of energy and shows that the electron is most likely transferred to the π^* orbital.[11] Electron transfer collisions differ from attachment of free electrons because of the presence of the donor atom, which in this case facilitates the π^*/σ^* symmetry-breaking deformation to produce acetate ion, lending credence to the theoretical calculations.[10] In the present experiments we study fluorine-substituted acetic acid, trifluoroacetic acid CF_3CO_2H (HFAc), which is a much stronger acid than acetic acid ($pK_A = 0.3$ vs 4.7) and has a larger dipole moment (2.28 vs 1.70), making it widely used in organic synthesis. It is found in the atmosphere where it arises from decomposition of various fluorocarbons and thermolysis of PTFE.[12] Its reactivity and high dipole moment make it attractive for further oriented molecule studies, and we report here electron transfer studies between K atoms and oriented HFAc molecules. For HFAc the fluoroacetate ion is the principal ion with a reactive cross section about the same as that of the acetate ion from HAc at the same center of mass energy. Fluoroacetate ion formation is favored by the positive-end approach ($-CO_2H$) and the electron is once again apparently transferred to the π^*_{CO} orbital. Fluorination provides new reaction channels that shed light on the electron transfer and subsequent decomposition of the transient negative ion.

Experimental Section

Potassium atoms are accelerated in a charge-exchange oven where the neutral atoms are ionized on a positively biased hot rhenium filament, accelerated toward a grounded slit a few tenths of a millimeter away, and allowed to charge exchange by drifting field-free through the neutral vapor. The beam emerging from the oven consists of neutrals (accelerated and thermal) and ions; charged plates deflect the ions and thermal atoms do not have enough energy to form ions. The beam of K atoms intersects a beam of HFAc produced by passing helium at ≈180 Torr over a liquid sample at 0 °C where the vapor pressure is ≈3 Torr.[13] The oven is heated to break up any dimers in the beam and temperatures ≈150 °C give optimal focused signals. But these experiments proved to be unusually difficult, perhaps because temperature fluctuations affect the reactivity via fluctuations in the rotational distribution.

The HFAc beam passes along the axis of an inhomogeneous 1.4 m hexapole electric field[14] where high-field seeking states are deflected toward the rods when charged to ±10 kV and low-field seeking states are deflected toward the axis and focused. For symmetric top molecules such as CH_3Br, the focused beam consists of molecules in M, K states such that $M^*K < 0$, and if these molecules are adiabatically transported into a uniform electric field, they are oriented in that field.

These molecules travel adiabatically from the hexapole field and intersect the atomic beam in a uniform field ≈300 V/cm defined by two identical and oppositely charged Wiley−McLaren TOF mass spectrometers.[15] The TOFMSs lie in the plane of the crossed beams and *E* is roughly along the relative velocity. The state-selected molecules are in low-field seeking states, and in this uniform field the negative end of the molecule points toward the negatively charged TOFMS. Reversing the polarity of the TOFMSs reverses *E* and the direction of orientation.

The beams are continuous and all voltages are constant so there is no time zero, but each electron transfer event produces an ion *pair simultaneously*. The positive ion signal starts a time to digital converter (TDC), and the negative ion signal (delayed 4 μs to allow detection of electrons) stops the TDC, giving the *difference* in flight times between the positive and negative ions. The mass spectrometers are identical, and the positive ion is

† Part of the "Vincenzo Aquilanti Festschrift".

* Corresponding author. E-mail: brooks@python.rice.edu.

10.1021/jp9029369
Published on Web 07/30/2009

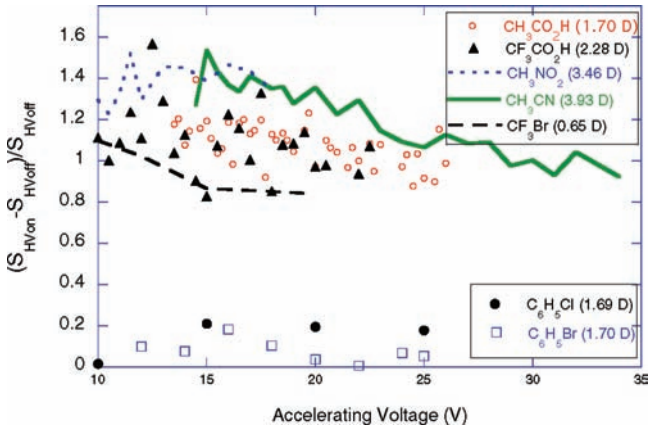

Figure 1. Increase in cross-beam signals relative to HV off signals for the most abundant ion using various molecular targets. Asymmetric tops with low barriers to internal rotation, HAc, HFAc, and CH_3NO_2 focus as well as symmetric tops, CF_3Br and CH_3CN. Asymmetric tops such as bromobenzene and chlorobenzene are almost unaffected by the high voltage on the focusing field.

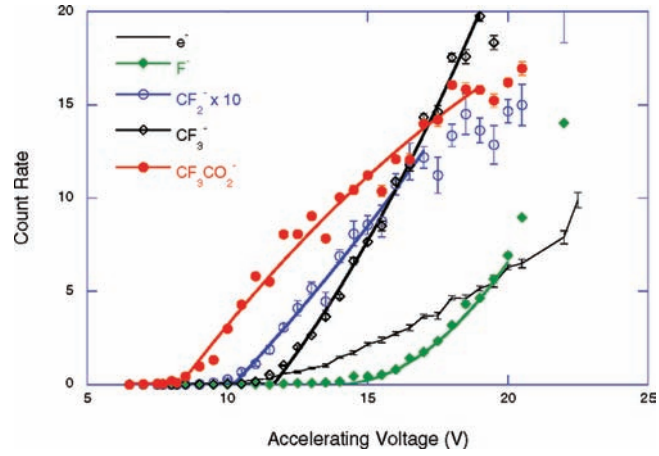

Figure 2. Average signals with HV on plotted vs accelerator voltage.

assumed to be K^+, so the time difference is a signature of the mass of the negative ion.

Coincidence tof spectra for each laboratory energy are acquired for positive or negative end attack with the hexapole field on and off for each orientation. If the hexapole field is off, a *randomly oriented* beam is transmitted, and its signal is used to eliminate any differences in collection or detection efficiency arising from different TOFMS polarities.[16] The experimental conditions are computer-controlled in random sequence.

Even though HFAc is an asymmetric top, the barrier to internal rotation is low, 242 cm^{-1},[17] and in these experiments it appears as a "symmetric top" with the $-CO_2H$ group effectively spinning about the CF_3. Other molecules with low barriers to internal rotation such as CH_3NO_2 (2 cm^{-1})[18] and acetic acid, CH_3CO_2H, HAc (170 cm^{-1}),[19] behave similarly. We show evidence that the molecule behaves as a "symmetric" top by showing the effect of the high voltage focusing field for several symmetric tops and several asymmetric tops in Figure 1. The gas beam intensities are not directly measured, but the ions produced in the electron transfer collision are *proportional* to the beam intensity. Thus the *relative* increase in signal when high voltage is applied to the focusing field $(S_{HVon} - S_{HVoff})/S_{HVoff}$, is proportional to the *relative* increase in beam intensity, $\Delta I/I$, where I is the beam intensity with HV off and ΔI the increase when the HV is on. For symmetric tops in our apparatus, the increase in crossed-beam ion signal, $S_{HVon} - S_{HVoff}$, is about the same as that with the high voltage off, S_{HVoff}, because the hexapole focuses molecules in low field seeking states. Clearly asymmetric tops with low barriers to internal rotation, HAc, HFAc, and CH_3NO_2 focus about as well as the true symmetric tops CF_3Br and CH_3CN. Asymmetric tops with no possibility for internal rotation to make them look "symmetric", such as bromobenzene or chlorobenzene, hardly focus at all.

The focusing characteristics thus strongly suggest that the HFAc molecules are oriented as a consequence of the internal rotation. If we approximate the internal rotation as being completely free and average the moments of inertia, I_B and I_C, we can treat the focusing and orientation as being from a symmetric top as reported in ref 16, finding $\langle -\cos\theta \rangle \approx 0.46$, somewhat smaller than the corresponding estimate for HAc,[11] 0.52. The dipole moment of the symmetrized HFAc molecule along the axis is $\mu_A = 1.70$ D, calculated from the average difference between the dipole direction in CF_3X and CH_3X (X = I, Br, Cl, and CN),[20] 2.56 D, and $\mu_A = 0.86$ for HAc.[19] This value of μ_A for HFAc, combined with $\mu_B = 1.47$ D from HAc, predicts that the dipole moment in HFAc is 2.24 D, in good agreement with the experimental value,[20] 2.28 ± 0.25 D, consistent with $-CO_2H$ being the positive end of the molecule. But this estimate of $\langle -\cos\theta \rangle$ is a rough approximation. Assuming free internal rotation is certainly justified for CH_3NO_2 with a 2 cm^{-1} barrier,[21] and possibly also for acetic acid. But the heavier fluorinated rotor lies deeper in the well of the hindering potential and free rotation seems less likely. The focusing of HFAc and the steric asymmetry of HFAc strongly resembles that of HAc, and we tentatively conclude that the orientation is comparable.

Results

Collisions between K atoms and HFAc molecules produce K^+ and the negative ions, F^-, CF_2^-, CF_3^-, $CF_2CO_2H^-$ and CF_3COO^- (FAc^-). Signals from these ions depend upon the hexapole focusing voltage and therefore arise from HFAc. Figure 2 shows the average ion signal intensities plotted vs the accelerating voltage in the charge exchange oven. Because absolute signals vary slightly from day to day, the thresholds listed in Table 1 are not determined from Figure 2 but are evaluated on a day-by-day basis for each polarity using signals with high voltage on S_{HVon}, high voltage off, S_{HVoff}, and the signal difference, ΔS. The average experimental thresholds are listed in Table 1. The electron signals arise mainly from background scattering. Very weak signals from $CF_2CO_2^-$ (<1 s^{-1}) are always <2% of the ion signal and are not shown in Figure 2.

The energy of the fast atoms differs slightly from the accelerating voltage in the charge exchange oven because of various contact potentials in the oven and a voltage drop along the rhenium filament and the energy scale must be calibrated. The threshold energy, E_{thresh}, is given by

$$E_{thresh} \geq IE + BDE - EA \quad (1)$$

where IE is the ionization energy of K, BDE is the bond dissociation of any bonds broken, and EA the electron affinity of the fragment receiving the electron. (The inequality applies if the fragments are internally excited.) The center-of-mass

TABLE 1: Ion Thresholds

	lab threshold[a]		
ion	expt	theory	neutrals
$CF_3CO_2^-$	8.47	6.16	H
$CF_2CO_2^-$	8.71		HF
CF_2^-	9.74	7.94	CO_2 + HF
		8.43	FCO_2H
		15.81	CO_2 + H + F
		15.66	CO_2H + F
		17.22	F + CO + OH
CF_3^-	11.17	8.36	CO_2H
		8.50	CO_2 + H
		9.92	CO + OH
F^-	13.89	8.37	CF_2CO_2H
		11.35	CF_2 + CO_2H
		11.49	CF_2 + CO_2 + H
	12.91		CF_2 + CO + OH
e^-	10.04	5.65	CF_3CO_2H

species	IE (eV)[13]	bond	BDE (eV)
K	4.34	CF_3-CO_2H	3.84[24]
F^-	3.40	CF_2-F	3.81[13]
CF_3^-	1.82	CO_2-H	0.11[25]
CF_2^-	0.18	OC−OH	1.16[25,26]
		HF	5.91[13]

$e^- + CF_3CO_2H \rightarrow CF_3CO_2^- + H$ BDE − EA = 0.38 eV[13]

[a] Experimental uncertainties are ≈±0.2 eV, theoretical ≈±0.1 eV.

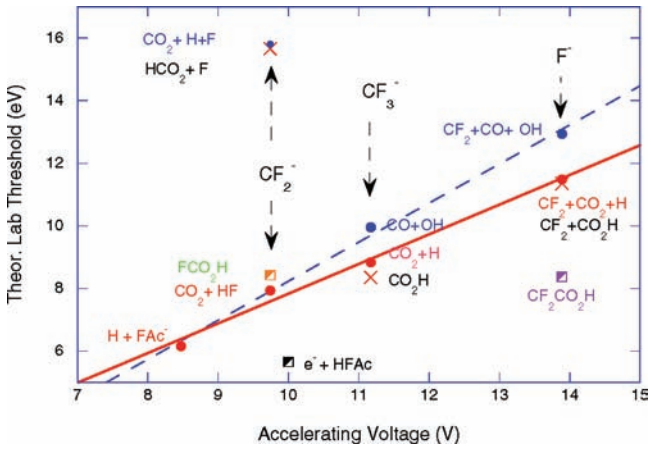

Figure 3. Theoretically calculated lab thresholds given in Table 1 plotted vs lab thresholds given in Table 1. For a given ion, different thresholds are possible depending on the neutral products listed next to the point. For example, CF_2^- with a lab threshold of 9.74 eV might have a theoretical (lab) threshold of 7.94, 8.43, 15.66, or 15.81 eV depending upon which neutral fragments are formed.

thresholds calculated from eq 1 are transformed to K lab energies using the relation

$$E_K = E_{thresh}(M/m_G) - E_G(m_K/m_G) \quad (2)$$

where M is the total mass of the colliding pair, m_K and m_G are the masses of K and gas, respectively, and E_G the energy of the gas beam calculated assuming a complete isenthalpic expansion in helium. This theoretical K lab energy is plotted vs the accelerating voltage as shown in Figure 3, giving a corrected K lab energy. Finally, the CM energy is calculated using eq 1 and the corrected K lab energy.

This procedure for calibrating the energy scale allows us to use different gases (with different CM-LAB transformations)

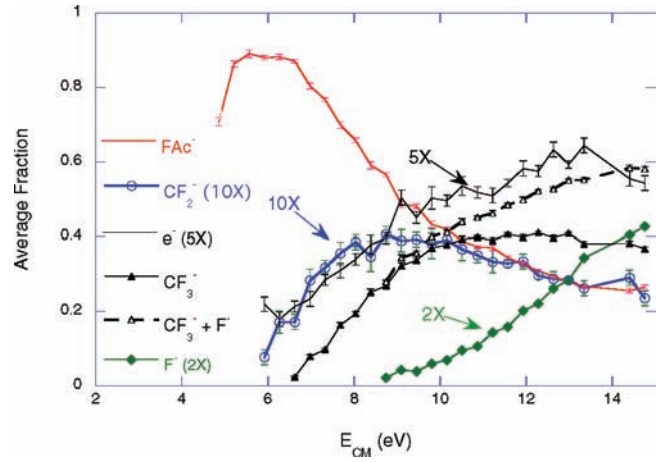

Figure 4. Average fraction of ions formed vs collision energy in the K + CF_3CO_2H center of mass system. The fractions from F^- and CF_2^- are enlarged for comparison.

but requires us to know threshold energies for the various ions, which in turn requires knowledge of the undetected neutral species. Several neutral channels exist for some of the ions, as shown in Table 1, and Figure 3 shows theoretical thresholds for various possible neutral products plotted against the experimental thresholds.

Even though we do not detect the neutral fragments in these experiments, we may still draw some conclusions about them. The fluoroacetate ion, FAc^- is formed together with an H atom. Comparison of the other radical anions shows that the experimental thresholds *increase* with radical electron affinity! Thus, formation of F^- must be accompanied by further fragmentation of the CF_2CO_2H moiety, probably forming H, CF_2, and CO_2 (or CF_2 and HOCO). The radical with the smallest electron affinity, CF_2, has a threshold ≈4 eV lower than F^-, even though two bonds must be broken to produce CF_2^-. This suggests that either a complex rearrangement in the neutral occurs to form FCOOH,[22,23] which does not require breaking of a second bond, or that strongly bound products HF + CO_2 are formed. The intermediate ion, CF_3^-, must produce H + CO_2 (or HOCO).

Figure 3 shows theoretical lab thresholds for various neutrals plotted against the accelerating voltage. Two calibration lines can be drawn depending on whether HOCO decomposes to OH + CO or to H + CO_2. These calibrations are statistically indistinguishable, but since the transient negative ion decays by first ejecting an H atom to form FAc^-, we favor the full curve corresponding to the channel forming H + CO_2. This is discussed more fully below. The threshold for electrons shown in Figure 3 (from HVon−HVoff data to emphasize HFAc contributions) is too high to yield ground state HFAc, but the threshold is too low for any fragmentation of the molecule. The electron apparently autodetaches from an excited parent molecule, suggesting that other ions could also result from parent molecules excited enough to cause further fragmentation of the neutrals. It thus seems likely that CF_3^- and F^- result from fragmentation of an excited FAc^{-}* from which the H atom had already departed, leaving only the CO_2 fragment as a possibility. Thus the solid line in Figure 3 is used to correct the applied voltage readings, and this corrected voltage is used to calculate the CM energy in subsequent discussion.

Figure 4 shows how the fraction of ions formed depends on collision energy. Fragmentation increases as the collision energy is increased. The transient negative ion, $HFAc^-$, initially loses an H atom to form FAc^-. Increasing collision energy apparently excites the transient $HFAc^-$, and at energies ≈5.5 eV, opens

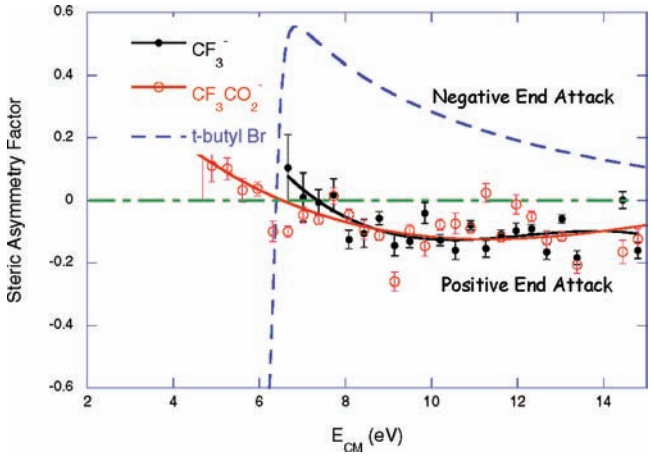

Figure 5. Steric asymmetry factors, G, for CF_3^- and FAc^-. Small, constant values of G are indicative of electron transfer to a π^* orbital, in contrast to G for *tert*-butyl bromide where the electron is transferred to a σ^* orbital. Curves are cubic fits to the data to guide the eye. Data above the dot-dashed line show a preference for negative end attack; data below show a preference for positive end attack.

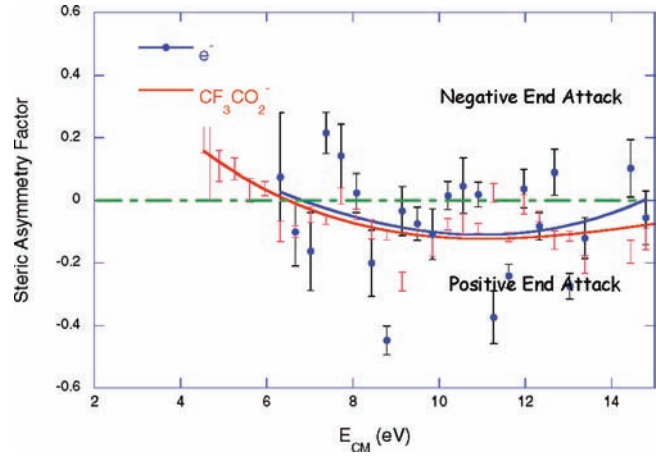

Figure 6. Steric asymmetry factors for formation of the electron compared with that for FAc^-. The electron data are fit with almost the same curve as that for FAc^-.

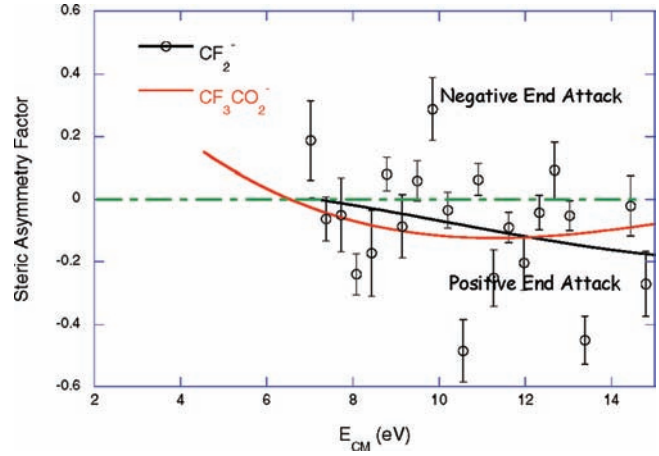

Figure 7. Steric asymmetry factors for CF_2^- compared to that for FAc^-.

channels to autodetachment and to complex rearrangement forming CF_2^-. At ≈6.5 eV the transient $HFAc^-$ is sufficiently excited to break the C−C bond to produce $CF_3^- + CO_2 + H$. A further increase in energy apparently produces excited CF_3^- that fragments into CF_2 and F^- near 9 eV.

The fate of the transient negative ion, $HFAc^-$, is thus complex. Initially, H can be ejected to form FAc^-, but as the energy of the $HFAc^-$ is increased to ≈5.5 eV, CF_2^- and autodetachment compete with FAc^-. Even though the neutral products are unknown, H atom loss cannot precede either autodetachment or CF_2^- formation because there is not enough energy to drive them sequentially. The FAc^- fragment initially formed can be sufficiently excited to break the C−C bond to form CF_3^- and increasing excitation produces excited CF_3^- that decomposes into $CF_2 + F^-$, as suggested in Figure 4 where the sum of F^- and CF_3^- signals is a monotonically increasing curve. We thus expect FAc^-, CF_2^-, and e^- to be formed competitively, but CF_3^- and F^- to be formed sequentially from FAc^-.

The effect of molecular orientation is given by the steric asymmetry factor, $G = (\sigma_- - \sigma_+)/(\sigma_- + \sigma_+)$, where $\sigma_\pm$ is the cross section for positive or negative end attack, which is evaluated from signals with hexapole HV on and HV off as previously described.[16] Figure 5 shows the steric asymmetry for the main products, FAc^- and CF_3^-. G would be zero if there were no difference in reactivity between the positive and negative ends or if the molecules were not oriented. Since G is not zero, we conclude that the molecules must be at least partially oriented. Reaction favors the positive end of the molecule (assumed to be $-CO_2H$) for energies >6.5 eV. The asymmetry for CF_3^- is almost exactly the same as that for FAc^-, which is expected if CF_3^- results from decomposition of FAc^- as we have suggested. The curves in Figure 5 are cubic fits to the data to guide the eye. The steric asymmetry factors for the other ions are scattered because the signals are much lower. The cubic fit for the electron signal in Figure 6 is almost the same curve as for FAc^-. The CF_2^- signal in Figure 7 only resembles the FAc^- fit, and the F^- steric asymmetry seems to be almost zero at energies >10 eV.

Discussion

The steric asymmetry factors for the principal products, FAc^- and CF_3^- are nonzero and show that the molecules are oriented. For $E \approx 9-15$ eV the value of G is ≈−0.1 whereas for a comparable energy range in HAc it is ≈+0.12, the difference being only in sign because the CO_2H end of the molecule changes polarity. In HAc the CO_2H end is negative and in HFAc the CO_2H end is positive.

Production of FAc^- for attack at the positive end is consistent with the electron being transferred to either the π^*_{CO} orbital or to the σ^*_{OH} orbital. We now consider these two possibilities.

Electron transfer to a σ orbital on atoms close to the molecular axis depends strongly on orientation and energy, as we have observed for CH_3Br,[15,16] t-C_4H_9Br,[16,27] CF_3Br,[28] and CF_3H.[29] This is illustrated by the values of G in Figure 5 for t-C_4H_9Br where the electron is transferred to a σ^* orbital. For energies several electronvolts above threshold, the effect of orientation is very small. As the energy is reduced, attack at the "wrong" end becomes less and less successful (compared to the "right" end) and the magnitude of G increases. G may even reverse sign[16,27,29,30] at energies *extremely* close to the threshold for separating the ions because the "right" end produces the ions close to one another and these ions will combine to give an undetected salt. Since the equilibrium position of the H atom in HFAc is likely between the oxygen atoms in the trans conformation, as is the case for formic acid[31] and acetic acid,[19] we would expect a similar steric asymmetry for HFAc if the electron were transferred to the σ_{OH} orbital.

On the other hand, the π^*_{CO} orbital is accessible from the side of the molecule. The orbital is "visible" in attack from either

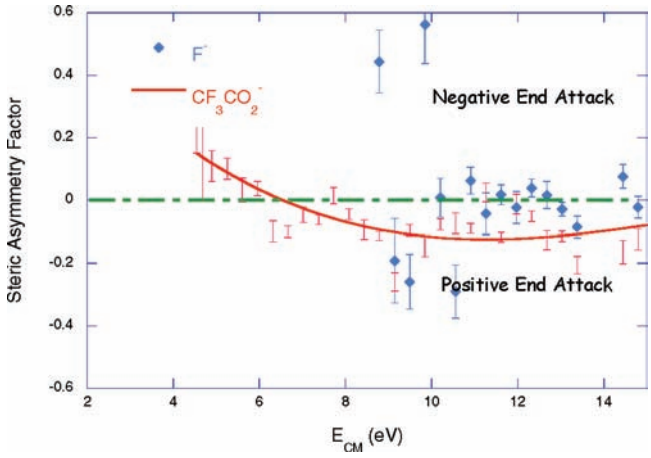

Figure 8. Steric asymmetry factors for F^- compared to FAc^-.

the CH_3 end or the CO_2H end and the steric asymmetry factor, *G*, is expected be small with a slight preference for the end containing the π^* orbital. Changing the collision energy will not change *G* very much because the orbital is always "visible". Electron transfer to π^* orbitals has been observed in CH_3CN,[32,33] CCl_3CN,[33] CH_3NC,[33] CH_3NO_2,[30,34] and CH_3CO_2H.[32] All of these molecules have by small, energy insensitive steric asymmetry parameters such as those for FAc^- and CF_3^- shown in Figure 5.

We thus conclude that FAc^- and CF_3^- are both preferentially produced by attacking the $-CO_2H$ end of the molecule with the electron initially entering the π^*_{CO} orbital. At energies <6 eV the steric asymmetry reverses sign and attack at the CF_3 end begins to favor formation of FAc^- possibly because low energy attack at the CO_2H end might not allow the nascent ions to separate.

Steric asymmetry factors for other ions are less definitive because the signals are smaller and the data are noisier. These are displayed in Figures 6−8 for completeness. Smooth curves (cubic fits) are drawn through the steric asymmetry factors for FAc^- and CF_3^- in Figure 5 to illustrate the overall trend of the data, and similar fits are plotted in Figures 6 and 7. The steric asymmetry factors for formation of the electron shown in Figure 6 are scattered, but the cubic fit is the same as that for FAc^- and for CF_3^-, mildly suggesting that these ions are all formed with the electron entering the π^*_{CO} orbital. The data for CF_2^- shown in Figure 7 are less convincing and show only that formation of CF_2^- could be consistent with π^* attack. The data for F^- are harder to interpret since there are wild swings and a region where the steric asymmetry is zero.

The attachment of *free* electrons to a molecule is different from the transfer of a bound atomic electron to a molecule, and comparison between these experiments helps explain both. For free electrons[35] the principal product is also FAc^-, but the similarity ends there. The free electrons attach in a resonance near 1 eV forming fluoroacetate FAc^- (and H) as well as $CF_2CO_2^-$ (and HF) and CF_2^- (and FCOOH). The intensities are comparable and in the ratio ≈1:0.8:0.4. The ions F^- and CF_3^- are produced with lower intensity at energies ≈7 eV. Electron *transfer* is not a resonant process above threshold, and Figure 4 shows that ion intensities depend on the energy. But it is clear from Figure 4 that at low energies FAc^- is the dominant product and that the other products observed in the electron attachment experiments, $CF_2CO_2^-$ and CF_2^- are formed in almost *negligible* amounts. These latter two ions are each formed in complex reactions requiring two bonds to be broken followed by a rearrangement of the atoms.

If the electron enters the π^*_{CO} orbital, migration to the σ^*_{OH} orbital is necessary to break the O−H bond, but that is symmetry forbidden (A″−A′) in the relaxed molecular geometry. In the free electron experiments only vibrationally excited molecules can break this symmetry, formation of FAc^- is inhibited, and decomposition must proceed to other channels to form $CF_2CO_2^-$ and CF_2^- as observed. These other products are absent in the present experiments, probably because the A″−A′ symmetry is broken by the nearby nascent K^+ ion. This makes breaking the O−H bond facile and robs these other channels of intensity. This symmetry breaking in HFAc and HAc is similar to that in CH_3CN where the electron initially enters the π^*_{CN} orbital but must migrate to the σ^*_{CC} bond to form CN^-. The ratio of CN^- to CH_2CN^- is vastly different in the electron transfer and electron attachment experiments, ≈100:1 for electron transfer,[32,33] but ≈1:100 for electron attachment.[36] The donor atom facilitates the Π−Σ surface crossing in CH_3CN, channeling the reactive flux into the production of more stable CN^-. In the attachment experiments, that interaction is absent, the Π−Σ surface crossing is not facile, the channel leading to CN^- is inhibited, and the reactive flux must proceed to another channel, formation of CH_2CN^-. Thus for the present case and in acetic acid, we expect the atomic donor to facilitate the surface crossing to an A′ surface yielding FAc^- or Ac^- at the expense of other products, and indeed it does. In effect, the donor atom opens the door to the low energy, but symmetry forbidden, channel.

We believe we have shown that the electron is transferred to the π^*_{CO} orbital in CF_3CO_2H as well as CH_3CO_2H[11] and that the donor atom breaks the symmetry in both cases to enable the OH bond to break. What implication does this have for the electron attachment experiments? It has recently been proposed that in formic acid (which we have not studied) the electron is attached via a very broad, higher energy, σ^*_{OH} shape resonance.[9,37] A similar mechanism could apply to the attachment of free electrons in HAc or HFAc, although it would seem that activating the OH bond would produce the respective acetate anions rather than the complex products observed.[5,35] Recent calculations[38] support the role of the π^* orbitals and it would appear that the comparative roles of the π^* and σ^* orbitals in attachment of free electrons is still an open question.

The electrons observed here have thresholds suggesting that they are autodetached from excited molecules. (Their detection in the free electron experiments is presumed difficult.) This suggests that the transient negative ion is formed with energy in excess of the minimum to break the O−H bond, leaving FAc^- in an excited state that can decompose to form CF_3^-, or at sufficiently high energies, CF_3^-* which then decomposes into F^-. The steric asymmetry for formation of CF_3^- is the same as that for FAc^- and roughly the same as for the autodetachment of the electron. Thus it is likely that the transient negative ion precursor for all three channels is the same and that donation of the electron to the π^*_{CO} orbital is the first step in the process, with the transient negative ion becoming increasingly excited as the energy of the incident atom is raised. In the free electron experiments this continual deposition of energy into the transient negative ion is not observed, suggesting that the electron donor may also play a role in exciting the transient negative ion.

Summary

Electrons jump from K atoms to oriented CF_3CO_2H molecules at low energies, producing K^+ ions and mainly trifluoroacetate (FAc^-) ions. FAc^- is favored by attack at the $-CO_2H$ end of the molecule, and the steric asymmetry suggests that the electron enters the π^*_{CO} orbital. The donor atom can perturb the transient

negative ion, allowing a symmetry forbidden migration of the electron to the σ^*_{OH} orbital and subsequent rupture of the O−H bond.

Electrons autodetach from the transient negative ion at energies above the autodetachment threshold, suggesting that the transient ion is excited. The electrons and other negative ion fragments, such as CF_3^-, appear with the same steric asymmetry as FAC^- implying that they all arise from transient negative ions formed by donation of the electron to the π^*_{CO} orbital.

Acknowledgment. We gratefully acknowledge financial support from the National Science Foundation. We thank Profs. Peter Harland and Bob Curl for helpful discussions, and Cesar Skalany for assistance in the laboratory.

References and Notes

(1) Boudaïffa, B.; Cloutier, P.; Hunting, D.; Huels, M. A.; Sanche, L. *Science* **2000**, *287*, 1658–1660.
(2) Simons, J. *Acc. Chem. Res.* **2006**, *39*, 772–779.
(3) Aflatooni, K.; Hitt, B.; Gallup, G. A.; Burrow, P. D. *J. Chem. Phys.* **2001**, *115*, 6489–6494.
(4) Pelc, A.; Sailer, W.; Scheier, P.; Probst, M.; Mason, N. J.; Illenberger, E.; Märk, T. D. *Chem. Phys. Lett.* **2002**, *361*, 277–284.
(5) Sailer, W.; Pelc, A.; Probst, M.; Limtrakul, J.; Scheier, P.; Illenberger, E.; Märk, T. D. *Chem. Phys. Lett.* **2003**, *378*, 250–256.
(6) Martin, I.; Skalicky, T.; Langer, J.; Abdoul-Carime, H.; Karwasz, G.; Illenberger, E.; Stano, M.; Matejcik, S. *Phys. Chem. Chem. Phys.* **2005**, *7*, 2212.
(7) Allan, M. *Phys. Rev. Lett.* **2007**, *98*, 123201-4.
(8) Allan, M. *J. Phys. B* **2006**, *39*, 2939–2947.
(9) Scheer, A. M.; Mozejko, P.; Gallup, G. A.; Burrow, P. D. *J. Chem. Phys.* **2007**, *126*, 174301-7.
(10) Rescigno, T. N.; Trevisan, C. S.; Orel, A. E. *Phys. Rev. Lett.* **2006**, *96*, 213201-4.
(11) Brooks, P. R. *J. Chem. Phys.* **2009**, *130*, 151102-4.
(12) Martin, J. W.; Mabury, S. A.; Wong, C. S.; Noventa, F.; Solomon, K. R.; Alaee, M.; Muir, D. C. G. *Environ. Sci. Technol.* **2003**, *37*, 2889–2897.
(13) NIST; NIST Standard Reference Database Number 69; 2003.
(14) Carman, H. S.; Harland, P. W.; Brooks, P. R. *J. Phys. Chem.* **1986**, *90*, 944–948.
(15) Harris, S. A.; Wiediger, S. D.; Brooks, P. R. *J. Phys. Chem.* **1999**, *103*, 10035–10041.
(16) Brooks, P. R.; Harris, S. A. *J. Chem. Phys.* **2002**, *117*, 4220–4232.
(17) Stolwijk, V. M.; van Eijck, B. P. *J. Mol. Spectrosc.* **1985**, *113*, 196–207.
(18) Tannenbaum, E.; Myers, R. J.; Gwinn, W. D. *J. Chem. Phys.* **1956**, *25*, 42–47.
(19) Krisher, L. C.; Saegebarth, E. *J. Chem. Phys.* **1971**, *54*, 4553–4558.
(20) *CRC Handbook of Chemistry and Physics*, 89th ed.; Lide, D. R., Ed.; CRC Press/Taylor and Francis: Boca Raton, FL, 2009; Internet Version, 2009.
(21) Jones, E. M.; Brooks, P. R. *J. Chem. Phys.* **1970**, *53*, 55–58.
(22) Havlas, Z.; Kovar, T.; Zahradnik, R. *J. Am. Chem. Soc.* **1985**, *107*, 7243–7246.
(23) Wiedmann, F. A.; Wesdemiotis, C. *J. Am. Chem. Soc.* **2002**, *116*, 2481–2485.
(24) Luo, Y.-R. *Handbook of Bond Dissociation Energies in Organic Compounds*; CRC Press: Boca Raton, FL, 2003.
(25) Duncan, T. V.; Miller, C. E. *J. Chem. Phys.* **2000**, *113*, 5138–5140.
(26) Yu, H.-G.; Poggi, G.; Francisco, J. S.; Muckerman, J. T. *J. Chem. Phys.* **2008**, *129*, 214307-9.
(27) Harris, S. A.; Brooks, P. R. *J. Chem. Phys.* **2001**, *114*, 10569–10572.
(28) Harland, P. W.; Brooks, P. R. *J. Am. Chem. Soc.* **2003**, *125*, 13191–13197.
(29) Jia, B.; Laib, J.; Lobo, R. F. M.; Brooks, P. R. *J. Am. Chem. Soc.* **2002**, *124*, 13896–13902.
(30) Brooks, P. R.; Harland, P. W.; Redden, C. E. *J. Phys. Chem. A* **2006**, *110*, 4697–4701.
(31) Kwei, G. H.; R. F. Curl, J. *J. Chem. Phys.* **1960**, *32*, 1592–1594.
(32) Harris, S. A.; Harland, P. W.; Brooks, P. R. *Phys. Chem. Chem. Phys.* **2000**, *2*, 787–791.
(33) Brooks, P. R.; Harland, P. W.; Harris, S. A.; Kennair, T.; Redden, C.; Tate, J. F. *J. Am. Chem. Soc.* **2007**, *129*, 15572–15580.
(34) Brooks, P. R.; Harland, P. W.; Redden, C. E. *J. Am. Chem. Soc.* **2006**, *128*, 4773–4778.
(35) Langer, J.; Stano, M.; Gohlke, S.; Foltin, V.; Matejcik, S.; Illenberger, E. *Chem. Phys. Lett.* **2006**, *419*, 228–232.
(36) Heni, M.; Illenberger, E. *Int. J. Mass Spectrom. Ion Processes* **1986**, *73*, 127–144.
(37) Gallup, G. A.; Burrow, P. D.; Fabrikant, I. I. *Phys. Rev. A* **2009**, *79*, 042701-7.
(38) Freitas, T. C.; Varella, M. T. d. N.; Costa, R. F. d.; Lima, M. A. P.; Bettega, M. H. F. *Phys. Rev. A* **2009**, *79*, 022706.

JP9029369